

BOLT: Block-Orthonormal Lanczos for Trace estimation of matrix functions

Kingsley Yeon
yeon@uchicago.edu

Promit Ghosal
promit@uchicago.edu

Mihai Anitescu
anitescu@mcs.anl.gov

Abstract

Efficient matrix trace estimation is essential for scalable computation of log-determinants, matrix norms, and distributional divergences. In many large-scale applications, the matrices involved are too large to store or access in full, making even a single matrix–vector (mat–vec) product infeasible. Instead, one often has access only to small subblocks of the matrix or localized matrix–vector products on restricted index sets. Hutch++ [27] achieves optimal convergence rate but relies on randomized SVD and assumes full mat–vec access, making it difficult to apply in these constrained settings. We propose the Block-Orthonormal Stochastic Lanczos Quadrature (BOLT), which matches Hutch++ accuracy with a simpler implementation based on orthonormal block probes and Lanczos iterations. BOLT builds on the Stochastic Lanczos Quadrature (SLQ) framework, which combines random probing with Krylov subspace methods to efficiently approximate traces of matrix functions, and performs better than Hutch++ in near flat-spectrum regimes. To address memory limitations and partial access constraints, we introduce Subblock SLQ, a variant of BOLT that operates only on small principal submatrices. As a result, this framework yields a proxy KL divergence estimator and an efficient method for computing the Wasserstein-2 distance between Gaussians—both compatible with low-memory and partial-access regimes. We provide theoretical guarantees and demonstrate strong empirical performance across a range of high-dimensional settings.

1 Introduction

Trace estimation is central to scalable machine learning, enabling approximation of log-determinants [5], matrix norms [18], distributional divergences, spectral densities [25], the Estrada index [38], and more [37]. In settings such as covariance estimation, kernel learning, and Gaussian processes, efficient trace estimation underlies key computational pipelines [6, 10, 39].

Recent randomized methods have made trace estimation highly efficient. Hutchinson’s estimator uses random sign probes and requires $O(1/\epsilon^2)$ matrix–vector products for additive error ϵ with high probability [3], while Hutch++ reduces this to $O(1/\epsilon)$ via low-rank sketching [27]. Non-adaptive sketching [21] improves memory and parallelism, establishing this rate as optimal. SLQ achieves fast convergence for analytic functions [36], and ContHutch++ generalizes to implicit operators [41]. However, many of these methods rely on spectral assumptions, require full matrix–vector products, and do not fully exploit sparsity.

Our work is motivated by estimating the KL divergence between mean-zero Gaussians in high-dimensional settings, where covariance matrices are large, possibly singular, and often inaccessible in full. These challenges arise in precision matrix estimation for Kalman filtering in weather data assimilation, where memory limits prohibit full matrix–vector products and the sample covariance is rank-deficient due to limited observations [14, 26, 16]. In such regimes, the KL divergence is not well-defined, motivating subblock-based approaches.

To address this, we propose Subblock SLQ—a memory-aware variant of BOLT that achieves fast convergence using only small principal submatrices. This method supports trace estimation without full matrix access at a time and remains effective even when the covariance is singular. Within this framework, we define a proxy KL divergence that remains meaningful without full-rank assumptions, enabling KL-based comparisons in sample-starved regimes. When KL is not required, the same estimator also supports the Wasserstein-2 (W_2) distance, which avoids matrix inversion and applies to any positive semidefinite covariance. Both estimators rely entirely on localized computations, making them ideal for large-scale, memory-constrained applications.

Our key contributions are as follows:

- (1) We develop the *Block-Orthonormal SLQ (BOLT)* algorithm, a block-based stochastic Lanczos quadrature method that achieves optimal $O(1/N_{\text{mv}})$ error decay in the number of matrix–vector products N_{mv} and the optimal number of FLOPS (see Table 1), without requiring spectral decay assumptions, matching Hutch++ [27]. Unlike Hutch++, BOLT avoids randomized SVD, making it easier to implement and more robust in flat-spectrum settings such as $\text{diag}(\text{Unif}[1, 2])$ (see Figure 3). BOLT leverages block probes well-suited to modern hardware and includes theoretical guarantees for unbiasedness and variance control (Theorem 2.1). Its computational benefits are demonstrated in Figure 2.
- (2) Building on BOLT, we propose the *Subblock SLQ* method for estimating divergences using only small principal submatrices, enabling fast and memory-efficient trace computation when full mat–vecs are infeasible. This method naturally supports both a proxy KL divergence and the Wasserstein-2 (W_2) distance, with accuracy and efficiency governed by localized matrix structure. Theoretical guarantees are provided in Algorithm 2, Theorem 3.3, and Lemma 3.2.
- (3) When the KL divergence is the target metric and the underlying covariance matrix is singular, we define a trace-based proxy for the KL divergence using Subblock SLQ, which is computable from small principal submatrices. This formulation remains well-defined even when the covariance matrix is singular. Lemma 3.4 shows that principal submatrices can retain full rank as long as their size does not exceed the rank of the full matrix, ensuring that the proxy KL divergence remains stable and tractable in regimes where the classical KL is undefined.
- (4) We validate the proposed proxy KL divergence as a practical metric through various experiments for assessing estimation error in low-sample regimes, particularly when the covariance matrix is singular and the classical KL divergence is undefined. To this end, we compare two strategies for estimating the Cholesky factor of the precision matrix: one that enforces sparsity on a lower-triangular factor L , and another that solves an unconstrained least-squares problem. The latter approach is ill-posed and yields substantial errors (Figure 13), which are accurately captured by our proxy KL divergence. Furthermore, we demonstrate that SLQ-KL regularization enhances generalization in low-rank learning tasks, including MNIST image classification (Figure 6), by promoting isotropy—a property known to improve generalization in both NLP and vision domains [2, 28, 7].

1.1 Related Works and Connections

Trace Estimation. Stochastic trace estimation is well-studied [27, 12, 3], with widely used methods such as Hutch++, XTrace, and XNysTrace offering effective variance reduction under favorable conditions. Hutch++, XTrace, and XNysTrace estimate the trace by sketching dominant eigenspaces, with XTrace and XNysTrace adding leave-one-out corrections using the exchangeability principle; these methods rely on full matrix–vector products and perform best under fast spectral decay, offering limited benefit for flat-spectrum matrices. XTrace and XNysTrace also incur higher computational overhead: their naïve implementations rely on repeated QR factorizations (XTrace) or SVDs (XNysTrace), costing $O(Nm^3)$ and $O(m^4)$, respectively, where m represents the number of matrix–vector products and N denotes the size of the matrix ($N \times N$). Optimized variants reduce this to $O(m^3)$ by exploiting a rank-one update structure, but still demand greater infrastructure than simpler estimators. Table 1 compares the implementations; see Appendix B for derivations and Table 2 for details.

Fuentes et al. [15] empirically observed that block probe vectors yield better accuracy than scalar ones and noted rapid convergence due to self-averaging, though no explicit convergence rate or variance bound was provided. Their analysis was limited to full-matrix settings with fixed block probes; they did not consider the role of orthogonalization, nor explore subblock strategies suitable for large-scale

Table 1: Flop counts to achieve ε -accuracy ($m, b \sim \Theta(\varepsilon^{-1})$) (**Optimized**).

Method	# Mat-vecs	Overhead (post-mat-vec)	Total flops
XTrace	m	$O(N m^2 + m^3)$	$O(N^2 m + N m^2 + m^3)$
XNysTrace	m	$O(N m^2 + m^3)$	$O(N^2 m + N m^2 + m^3)$
Hutch++	m	$O(N m^2)$	$O(N^2 m + N m^2)$
BOLT	m	$O(N m^2)$	$O(N^2 m + N m^2)$

or structured matrices. None of these methods explicitly address memory usage or scalability under storage constraints, which are often critical in high-dimensional applications.

In a similar spirit as block SLQ, sliced-Wasserstein (SW) distances provides the framework to compute distance between two probability measure by projecting measures onto random lines:

$$\text{SW}_p^p(P, Q) = \int_{\mathbb{S}^{d-1}} W_p^p(P_\theta, Q_\theta) d\theta,$$

where P_θ, Q_θ are 1D marginals of P, Q along θ [30, 22]. For example, if $P = \mathcal{N}(0, uu^T)$, $Q = \mathcal{N}(0, vv^T)$ are rank-one Gaussians, projections orthogonal to both u and v collapse to the origin, yielding zero SW distance despite distinct inputs. Empirically, SW distances are estimated via Monte Carlo integration:

$$\widehat{\text{SW}}_p^p(P, Q) = \frac{1}{L} \sum_{\ell=1}^L W_p^p(P_{\theta_\ell}, Q_{\theta_\ell}),$$

with $O(L^{-1/2})$ convergence [29], improvable to $O(L^{-3/4})$ with spherical harmonics control variates (SHCV) [31]. However, unlike block SLQ variants, SW methods degrade in high dimensions and do not exploit matrix sparsity or structure.

1.2 Notation

Vectors are lowercase (e.g., x, y); matrices are uppercase (e.g., A, Σ), with transpose A^T . For $A \in \mathbb{S}_+^n$, let $\lambda_i(A)$ be its eigenvalues in decreasing order. We write $\|A\|$, $\|A\|_F$, and $\text{tr}(A)$ for the spectral norm, Frobenius norm, and trace, respectively. \mathbb{S}_+^n denotes the cone of symmetric positive semidefinite $n \times n$ matrices. $\mathcal{N}(\mu, \Sigma)$ is the Gaussian with mean μ and covariance Σ . For $S \subset \{1, \dots, n\}$, $A_S = A(S, S)$ is the submatrix of A indexed by S , and P_S projects onto $\{e_i : i \in S\}$. We write $A \preceq B$ to mean $B - A$ is positive semidefinite.

Expectations and variances are denoted $\mathbb{E}[\cdot]$, $\text{Var}[\cdot]$, and $\|x\|$ is the Euclidean norm.

1.3 KL Divergence of Gaussians as a Trace Problem

The KL divergence between Gaussians $p = \mathcal{N}(\mu_1, \Sigma_1)$ and $q = \mathcal{N}(\mu_2, \Sigma_2)$, with $\mu_1 = \mu_2 \in \mathbb{R}^d$ and $\Sigma_1, \Sigma_2 \in \mathbb{S}_+^d$, simplifies to $D_{\text{KL}}(p \parallel q) = \frac{1}{2}[\text{tr}(\Sigma_2^{-1}\Sigma_1) + \text{tr}(\log \Sigma_1) - \text{tr}(\log \Sigma_2) - d]$ [1, 17, 16, 24, 13, 33]. Letting $\Sigma_2^{-1} = LL^T$ (e.g., from PDE-generated covariances or Vecchia approximations [15, 16]) and $\Sigma = \Sigma_1$, this becomes $D_{\text{KL}} = \frac{1}{2} \text{tr}(f(LL^T\Sigma))$ where $f(\lambda) = \lambda - \log \lambda - 1$. To approximate $\text{tr}(f(A))$, we use Hutchinson’s method [19] with i.i.d. Gaussian probes $g_i \sim \mathcal{N}(0, I)$:

$$\text{tr}(f(A)) \approx \frac{1}{q} \sum_{i=1}^q g_i^T f(A) g_i.$$

Applying Lanczos quadrature [36, 4] to each g_i , we construct a tridiagonal matrix T_i , diagonalize $T_i = U_i \Lambda_i U_i^T$, and obtain $\sum_{j=1}^k w_{ij} f(\mu_{ij})$ where $w_{ij} = (U_i)_{1j}^2$. Our estimator is

$$\widehat{D}_{\text{KL}}(f(A)) := \frac{1}{2q} \sum_{i=1}^q \sum_{j=1}^k w_{ij} f(\mu_{ij}).$$

1.4 Wasserstein-2 Distance as a Trace Problem

For Gaussians $p = \mathcal{N}(\mu, \Sigma_1)$, $q = \mathcal{N}(\mu, \Sigma_2)$, the squared Wasserstein-2 distance is given by $W_2^2(p, q) = \text{tr}(\Sigma_1 + \Sigma_2) - 2\tau$ where $\tau := \text{tr}((\Sigma_1^{1/2}\Sigma_2\Sigma_1^{1/2})^{1/2})$. Noting $\text{Spec}(\Sigma_1^{1/2}\Sigma_2\Sigma_1^{1/2}) = \text{Spec}(\Sigma_2\Sigma_1)$ under the assumption that $\Sigma_1 \in \mathbb{S}_+^n$, since $\Sigma_2\Sigma_1 = \Sigma_1^{-1/2}(\Sigma_1^{1/2}\Sigma_2\Sigma_1^{1/2})\Sigma_1^{1/2}$, define $B = \Sigma_2\Sigma_1$, so that $\text{tr}((\Sigma_1^{1/2}\Sigma_2\Sigma_1^{1/2})^{1/2}) = \text{tr}(f(B))$ with $f(x) = \sqrt{x}$.

Applying stochastic Lanczos quadrature on B (no explicit square roots required): for $i = 1, \dots, q$, draw g_i , run k Lanczos steps to get the tridiagonal $T_i = U_i \Theta_i U_i^T$, where $\Theta_i = \text{diag}(\theta_{i1}, \dots, \theta_{ik})$, and compute $g_i^T f(B) g_i \approx e_1^T f(T_i) e_1 = \sum_{j=1}^k w_{ij} \sqrt{\theta_{ij}}$, with $w_{ij} = (U_i)_{1j}^2$. Then $\hat{\tau} = \frac{1}{q} \sum_{i=1}^q \sum_{j=1}^k w_{ij} \sqrt{\theta_{ij}}$, and $W_2^2(p, q) \approx \text{tr}(\Sigma_1 + \Sigma_2) - 2\hat{\tau}$. The trace term $\text{tr}(\Sigma_1 + \Sigma_2)$ can also be efficiently estimated using BOLT, requiring only matrix–vector products with Σ_1 and Σ_2 .

2 Block-Orthonormal Stochastic Lanczos Quadrature

We introduce the Block-Orthonormal Stochastic Lanczos Quadrature (BOLT) method, a randomized trace estimator that avoids the high overhead of XTrace [12] and the projection step used in Hutch++ [27]. While Hutch++ requires a randomized SVD and assumes fast spectral decay, BOLT applies Lanczos directly to orthonormal blocks, achieving the same convergence rate without low-rank assumptions. A related idea of using designed probing for Gaussian processes was explored in [34], which observed improved empirical performance but did not analyze the asymptotic behavior of the estimator. We present BOLT in Algorithm 1 and compare its FLOP costs to other stochastic trace estimators in detail in Appendix B. All code to reproduce the figures can be found at <https://github.com/chebyshevtech/BOLT>.

Algorithm 1 Block-Orthonormal SLQ (BOLT): Randomized Estimation of $\text{tr}(f(A))$

- 1: **Input:** Symmetric matrix or operator A , analytic function f , number of probes q , Lanczos steps k , block size b .
 - 2: **(KL case):** set $A = L^T \Sigma L$, $f(\lambda) = \lambda - \ln \lambda - 1$.
 - 3: **for** $i = 1, \dots, q$ **do**
 - 4: Draw $Z_i \in \mathbb{R}^{n \times b}$ with either Rademacher or standard Gaussian entries, and orthonormalize to obtain V_i .
 - 5: Run block Lanczos on A starting from V_i for k steps to form tridiagonal T_i .
 - 6: Diagonalize $T_i = U_i \text{diag}(\mu_{i1}, \dots, \mu_{ikb}) U_i^T$.
 - 7: Compute weights $w_{ij} = \sum_{r=1}^b (U_i)_{rj}^2$ and $\eta_i = \sum_{j=1}^{kb} w_{ij} f(\mu_{ij})$.
 - 8: **end for**
 - 9: $\hat{\text{tr}}(f(A)) = \frac{n}{qb} \sum_{i=1}^q \eta_i$.
 - 10: **Output:** $\hat{\text{tr}}(f(A))$ (or for KL, $\hat{D}_{\text{KL}} = \frac{1}{2} \hat{\text{tr}}(f(A))$).
-

The SLQ method which was [4] combines Hutchinson probing with Gaussian quadrature. Rather than computing the full matrix at $O(n^3)$ cost where n denotes the size of the matrix, SLQ uses qk matrix–vector products [23] for certain choice of q and k . It was later shown that for any fixed q , $k = O(\ln n / \sqrt{\epsilon})$ Lanczos steps can yield a precision of order ϵ . Our approach, motivated by block SLQ based method of [15] introduces a block-orthonormal SLQ variant for improved convergence.

To rigorously quantify the performance of our estimators, we now present formal theoretical results establishing unbiasedness, variance bounds, and exact recovery guarantees under appropriate sampling conditions. These results not only underpin the empirical observations reported in later sections but also highlight the fundamental differences between block and scalar probing strategies. Full proofs of the following theorems and lemmas are deferred to Appendix A, specifically Sections A.1 and A.2.

Theorem 2.1 (Block SLQ Estimator). *Let $A \in \mathbb{R}^{n \times n}$ be symmetric positive semidefinite with eigenvalues $\{\lambda_i\}_{i=1}^n$, and let $f : [0, \infty) \rightarrow \mathbb{R}$ be convex and twice continuously differentiable. For each of q independent trials, generate an $n \times b$ random matrix V with orthonormal columns*

($\mathbb{E}[VV^T] = \frac{b}{n}I_n$) and define $X(V) := \frac{n}{b} \operatorname{tr}(V^T f(A)V)$. The Monte Carlo estimator

$$\hat{T} := \frac{1}{q} \sum_{i=1}^q X(V_i)$$

satisfies:

1. $\mathbb{E}[X(V)] = \operatorname{tr}(f(A))$. (If $b = n$, then $VV^T = I_n$ and $X(V)$ is exact.)
2. The variance is

$$\operatorname{Var}[X(V)] = \frac{2n}{b(n+2)} \left(1 - \frac{b-1}{n-1}\right) \left(\sum_{i=1}^n f(\lambda_i)^2 - \frac{1}{n} (\operatorname{tr}(f(A)))^2\right),$$

and

$$\operatorname{Var}[\hat{T}] = \frac{1}{q} \operatorname{Var}[X(V)].$$

3. If $X(V) \in [\ell_{\min}, \ell_{\max}]$ almost surely, then for any $\varepsilon > 0$,

$$\mathbb{P}\left(|\hat{T} - \operatorname{tr}(f(A))| \geq \varepsilon\right) \leq 2 \exp\left(-\frac{2q\varepsilon^2}{(\ell_{\max} - \ell_{\min})^2}\right),$$

so that with probability at least $1 - \delta$,

$$|\hat{T} - \operatorname{tr}(f(A))| \leq (\ell_{\max} - \ell_{\min}) \sqrt{\frac{\ln(2/\delta)}{2q}}.$$

Computationally, it is desirable to compare the relative error of estimators as a function of the number of matrix–vector products N_{mv} . The following result shows that our proposed orthogonal block stochastic Lanczos quadrature estimator achieves an $O(1/N_{\text{mv}})$ decay rate, matching Hutch++, in contrast to the $O(N_{\text{mv}}^{-1/2})$ rate of standard Hutchinson (scalar SLQ). In block SLQ, we fix the number of probes $q = 1$ and increase the block size with the mat–vec budget, whereas scalar SLQ uses a fixed block size $b = 1$ and averages over many independent probes. The next lemma formalizes these decay rates under a fixed mat–vec budget. We assume the underlying matrix has *flat spectrum*, meaning that for all eigenvalues $\lambda_i, \lambda_j \in \operatorname{Spec}(A)$ for $A \in \mathbb{R}^{n \times n}$, the spectral variation is bounded by $|\lambda_i - \lambda_j| < d$, where $0 \leq d \leq \varepsilon n$, for some $\varepsilon > 0$.

Lemma 2.2 (Error-Decay Rates vs. Mat–Vec Budget). *Let $A \in \mathbb{R}^{n \times n}$ and $f : [0, \infty) \rightarrow \mathbb{R}$ be the same as in Theorem 2.1. Let us define $B := f(A)$ with eigenvalues $f(\lambda_1), \dots, f(\lambda_n)$. Denote $T = \operatorname{tr}(B)$. Suppose we budget N_{mv} matrix–vector product for Block SLQ which uses one probe of block size $b = \lfloor N_{\text{mv}}/2 \rfloor$. Define $\hat{T}_{\text{block}} := \frac{n}{b} \operatorname{tr}(V^T B V)$, where $V \in \mathbb{R}^{n \times b}$, $V^T V = I_b$. Then we have*

$$|\hat{T}_{\text{block}} - T| = O(N_{\text{mv}}^{-1}).$$

Remark 2.1. It is worth noting that if one uses the block size $b = 1$ in Lemma 2.2, then the Block SLQ reduces to the Scalar SLQ Hutchinson estimator of [4] which is known to converge at rate $O(N_{\text{mv}}^{-1/2})$.

We now numerically demonstrate KL divergence estimation between two zero-mean Gaussians, where $A = \Sigma \in \mathbb{R}^{200 \times 200}$ is a Gaussian RBF kernel with $\sigma = 2$, and LL^T is the Cholesky factor of the precision matrix. Figure 1 compares wall-clock runtimes: SLQ- and Hutchinson-based estimators scale efficiently with matrix size, unlike direct log-det computation. Figure 2 shows convergence consistent with Lemma 2.2: scalar SLQ decays at $O(1/\sqrt{N_{\text{mv}}})$, while Hutch++ and Block SLQ achieve the optimal $O(1/N_{\text{mv}})$ rate.

Unlike Hutch++ [27], which first multiplies the matrix of interest A by a sketching matrix S (a randomized matrix with independent Gaussian or Rademacher entries) to form a sketch AS and then performs a QR-decomposition of AS to approximate the top eigenspace, our block SLQ method takes a simpler route: we draw a single Rademacher or Gaussian block $Z \in \mathbb{R}^{n \times b}$, compute its QR factorization $Z = \tilde{Q} \tilde{R}$, and use the orthonormal columns of \tilde{Q} directly as our block probe—without

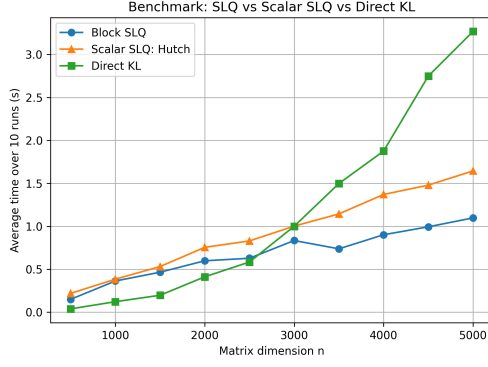


Figure 1: Timing comparisons

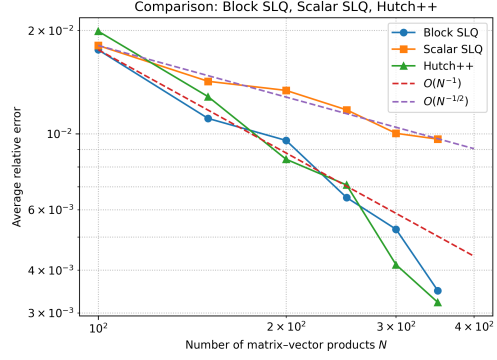


Figure 2: Relative error (KL divergence) vs. number of matrix–vector products (Scalar-Hutch vs. Block SLQ) vs. Hutch++

any prior multiplication by A . This minor change still induces negative covariances between the quadratic forms $v_r^T f(A) v_r$, since orthogonal directions naturally “self-correct”: overestimation by one vector implies underestimation by its orthogonal complement.

Figure 3 shows this effect for $A = \text{diag}(d)$ with $d_i \sim \text{Unif}[1, 2]$. Hutch++ builds a sketch $Q \in \mathbb{R}^{n \times s}$ with $s = N_{\text{mv}}/3$, computes $\text{tr}(Q^T A Q)$ exactly, and estimates the remainder with $g = N_{\text{mv}} - s$ Monte Carlo probes, yielding $O(g^{-1/2}) = O(N_{\text{mv}}^{-1/2})$ error. Block SLQ instead draws one orthonormal block $\tilde{Q} \in \mathbb{R}^{n \times b}$ and computes $\hat{T} = \frac{n}{b} \sum_{j=1}^b d_{k_j}$.

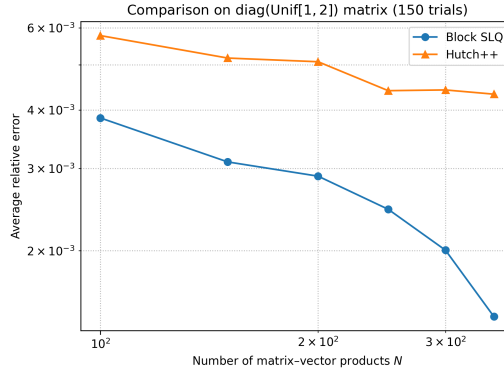


Figure 3: BOLT outperforms Hutch++ in approximating the trace of $\text{diag}(\text{Unif}[1, 2])^2$ (150 trials)

3 Sub-block Stochastic Lanczos Quadrature

The goal of this section is address the trace estimation of matrix functions when the matrix vector product computation of the full matrix is unavailable or too expensive. We seek to propose a consistent trace estimation method which works under the assumption when the matrix vector product subblocks are available. Using the the following result (proved in Appendix A.4 and A.5), we propose a unified estimator (Algorithm 2) that applies even when $A = L^T \Sigma L$ is singular or Σ is large and sparse, relying on small submatrices instead of full matrix–vector products to approximate $\text{tr}(f(A))$.

Lemma 3.1 (Full Coverage via Block Sampling). *Let $A \in \mathbb{R}^{n \times n}$. For $1 \leq s < n$, suppose one independently samples t subblocks where each random subblock is an s -subset chosen randomly without replacement $\{1, \dots, n\}$. Then if*

$$t \geq \frac{n}{s} \log\left(\frac{n}{\epsilon}\right),$$

the union of indices covers $\{1, \dots, n\}$ with probability at least $1 - \epsilon$.

We now formalize the correctness of the sub-block based trace estimation.

Lemma 3.2 (Unbiased Subblock Trace Estimation and Exact Recovery under Full Coverage). *Let $A \in \mathbb{R}^{n \times n}$ be symmetric positive semidefinite and $f: [0, \infty) \rightarrow \mathbb{R}$ nondecreasing. For any subset $S \subset \{1, \dots, n\}$ with $|S| = s$, define*

$$X(S) := \frac{n}{s} \text{tr}(f(A)_S).$$

See section 1.2 for $f(A)_S$. Then $\mathbb{E}_S[X(S)] = \text{tr}(f(A))$ and, since each $\text{tr}(f(A)_S) \leq \text{tr}(f(A))$, the estimators converge from below. Moreover, if S_1, \dots, S_t are independently sampled and their union U covers $\{1, \dots, n\}$, then

$$\text{tr}(f(A)_U) = \text{tr}(f(A)).$$

Figure 4 illustrates this recovery empirically: we construct $A = B^T B$ with $B \sim \mathcal{N}(0, 1)^{n \times n}$, and estimate $\text{tr}(A)$ by averaging scaled traces over t random subblocks of size $s = 10$. When $t \geq \frac{n}{s} \log(\frac{n}{\varepsilon})$, the estimate approaches the true trace with probability at least 0.9.

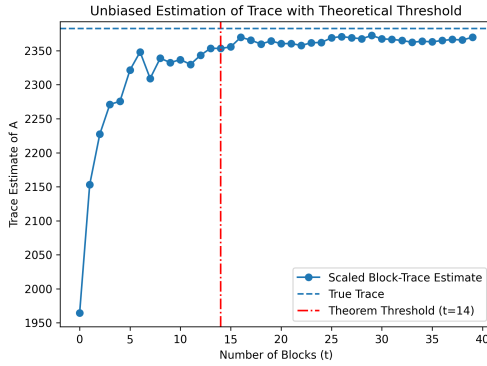


Figure 4: Trace recovery under Lemma 3.2, $t \geq \frac{n}{s} \log(\frac{n}{\varepsilon})$; $n = 50$, $s = 10$, $\varepsilon = 0.1$.

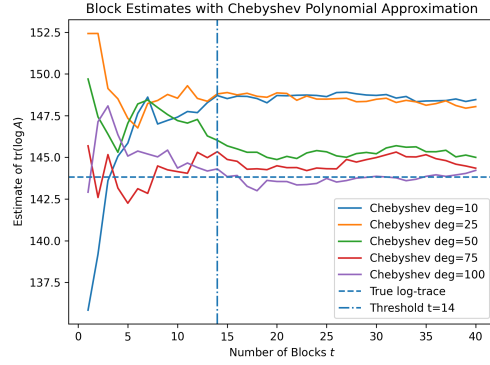


Figure 5: Polynomial localization.

When A is too large or singular to apply $f(A)$ directly, we instead approximate $f(A_S)$ using local computations. The next result (proved in A.6) ensures this approximation is valid for polynomial filters:

Theorem 3.3 (Exact Localization of Polynomial Filters on Principal Subblocks). *Let $A \in \mathbb{R}^{n \times n}$ have sparsity pattern inducing a graph G , and assume $\text{spec}(A) \subset [\lambda_{\min}, \lambda_{\max}]$. Let p_m be a degree- m Chebyshev polynomial approximating f with uniform error ε . For any subset S , define*

$$S_r := \{v : \text{dist}_G(v, S) \leq r\}.$$

If $r \geq m$, then

$$[p_m(A)]_{S,S} = [p_m(A_{S_r, S_r})]_{S,S} = p_m(A_S).$$

Moreover, the trace approximation error on S satisfies

$$|\text{tr}(f(A)_S) - \text{tr}(f(A_S))| \leq 2s\varepsilon.$$

Remark 3.1. In practice, we do not construct p_m explicitly. Instead, block Lanczos or Gaussian quadrature implicitly builds such filters and integrates polynomials exactly up to degree $2k - 1$ with k iterations.

Figure 5 confirms this localization. Such localization techniques have been widely employed in convolutional neural networks for graph filtering [8]. An alternative approach to stochastic Lanczos quadrature is to approximate the matrix logarithm using a deep polynomial representation [40], designed to minimize the number of matrix multiplications needed for accurate reconstruction [20].

3.1 Applications of Proxy KL Divergence

In this subsection, we will define the proxy KL divergence and explore its applicability in two ways. First, we verify that in the low sample regime, sparsity in the Cholesky factor of the precision

Algorithm 2 Unified Block SLQ: Randomized Estimation of $\text{tr}(f(A))$

```

1: Input: Symmetric matrix/operator  $A$ , analytic  $f$ , probes  $q$ , subblocks  $t$ , block size  $s$ , steps  $k = s$ ,
   tol.  $\varepsilon$ .
2: Compute effective dimension  $r_{\text{eff}} = \#\{i : A_{ii} > \varepsilon\}$ .
3: if  $t = 1$  or  $r_{\text{eff}} \leq s$  then
4:   Reduce to Algorithm 1
5: end if
6: Sample subblocks  $S_1, \dots, S_t \subset \{1, \dots, r_{\text{eff}}\}$ , each of size  $s$ .
7: for  $i = 1, \dots, t$  do
8:   Form  $A_{S_i} = A(S_i, S_i)$ .
9:   for  $j = 1, \dots, q$  do
10:    Draw  $Z_{ij} \in \mathbb{R}^{s \times b}$  with either Rademacher entries ( $\pm 1$ ) or standard Gaussian entries, and
       orthonormalize to obtain  $V_{ij}$ .
11:    Run block Lanczos on  $A_{S_i}$  from  $V_{ij}$  for  $k$  steps to get  $T_{ij}$ .
12:    Diagonalize  $T_{ij} = U_{ij} \text{diag}(\mu_{ij1}, \dots, \mu_{ij,ks}) U_{ij}^T$ .
13:     $\eta_{ij} = \sum_{l=1}^{ks} (\sum_{r=1}^s (U_{ij})_{rl}^2) f(\mu_{ijl})$ .
14:   end for
15:    $\eta_i = \frac{1}{q} \sum_{j=1}^q \eta_{ij}$ .
16: end for
17:  $\widehat{\text{tr}}(f(A)) = \frac{r_{\text{eff}}}{ts} \sum_{i=1}^t \eta_i$ .
18: Output:  $\widehat{\text{tr}}(f(A))$  (for KL,  $\widehat{D}_{\text{KL}} = \frac{1}{2} \widehat{\text{tr}}(f(A))$ ).

```

matrix is necessary to produce accurate results. Second, we use our proxy KL as a regularizer for the classification of MNIST data. In both cases, the matrix of interest is singular; therefore, the regular KL divergence is not defined. One such instance arises for the sample covariance $\widetilde{\Sigma} = \sum_{i=1}^m u_i u_i^T$, with $u_i \sim \mathcal{N}(0, \Sigma)$ and $m \ll n$. Notice that $\widetilde{\Sigma}$ is singular, even though the true covariance Σ is full rank. This makes $\log(\widetilde{\Sigma})$ and the standard KL divergence ill-defined. We introduce a *proxy KL divergence* via trace functionals on subblocks of $\widetilde{\Sigma}$, which remains well-posed in singular, sample-starved settings and applies to any symmetric matrix, regardless of rank or access.

Lemma 3.4 (Subblock full-rankness from Wishart sampling). *Let $\Sigma \in \mathbb{R}^{n \times n}$ be positive definite, and let $u_1, \dots, u_m \sim \text{iid } \mathcal{N}(0, \Sigma)$. Define the sample covariance (unnormalized) $\widetilde{\Sigma} = \sum_{i=1}^m u_i u_i^T$, which has rank at most m . Fix any index set $S \subset \{1, \dots, n\}$ of size $s \leq m$, and let $P_S \in \{0, 1\}^{n \times s}$ be the coordinate-selection matrix picking those s rows. Then the $s \times s$ subblock $\widetilde{\Sigma}_S = P_S^T \widetilde{\Sigma} P_S$ follows the central Wishart distribution $W_s(P_S^T \Sigma P_S, m)$. Since $m \geq s$ and $P_S^T \Sigma P_S$ is invertible, $\widetilde{\Sigma}_S$ is almost surely invertible and hence $\text{rank}(\widetilde{\Sigma}_S) = s$.*

Although $\widetilde{\Sigma} = \sum_{i=1}^m u_i u_i^T$ is rank-deficient when $m < n$, its subblocks $\widetilde{\Sigma}_S$ are full rank with probability one whenever $s \leq m$, a property inherited from the Wishart structure (Lemma 3.4, proved in A.3). For stable KL estimation, one must choose subblocks with $s \leq m$; beyond this threshold, $\widetilde{\Sigma}_S$ becomes singular (Figure 10). Appendix C discusses this transition further, including smallest eigenvalue statistics from Edelman [11] and universality extensions by Tao and Vu [35].

Definition 3.5 (Proxy KL Divergence). *Let $A \in \mathbb{R}^{n \times n}$ be symmetric positive semidefinite (possibly singular) and define*

$$f(\lambda) := \lambda - \log \lambda - 1.$$

For any subset $S \subset \{1, \dots, n\}$ with $|S| = s$, let $f(A)_S$ denote the $s \times s$ subblock of $f(A)$ indexed by S . The proxy KL divergence is then

$$\widehat{D}_{\text{KL}}^{\text{proxy}}(f(A)) := \frac{1}{t} \sum_{i=1}^t \widehat{D}_{\text{KL}}(f(A)_{S_i})$$

where S_1, \dots, S_t are independent sub-blocks sampled randomly from the set $\{1, \dots, n\}$ without replacement.

Notice that $\mathbb{E}[\frac{n}{s} \text{tr}(f(A)_S)] = \text{tr}(f(A))$ by Lemma 3.2. Hence $\widehat{D}_{\text{KL}}^{\text{proxy}}$ is an unbiased estimator of the true KL divergence $\frac{1}{2} \text{tr}(f(A))$.

We illustrate our algorithm with two examples. First, we apply Algorithm 2 to estimate both the standard KL divergence in the full-rank case and a proxy KL divergence when the matrix is singular. Figures 12 and 13 in appendix E show this behavior under least-squares and sparsity-constrained Cholesky factorizations. Without sparsity in L , the error matrix $E = LL^T \Sigma$ has $\|E\|_F = 2 \times 10^{14}$, matching the proxy KL divergence and indicating poor approximation. Enforcing sparsity in L sharply reduces this error, as reflected in the KL metric.

Second, we train an MLP (input $784 \rightarrow$ hidden $8 \rightarrow$ output 10) on MNIST [9] with batch size 4. At each step, we compute hidden activations $H \in \mathbb{R}^{4 \times 8}$, center them to H_c , and form the empirical covariance $\Sigma = \frac{1}{3} H_c^T H_c \in \mathbb{R}^{8 \times 8}$. Since Σ is singular, standard KL regularization is undefined. We instead apply the SLQ-KL penalty $\frac{\beta}{2} \text{tr}(f(\Sigma))$ via subblock SLQ to encourage isotropy, a property known to aid generalization in NLP and vision [2, 28, 7]. Figure 6 shows improved test accuracy with $\beta = 0.01$; Figure 7 highlights corrected misclassifications. See Appendix D for full setup.

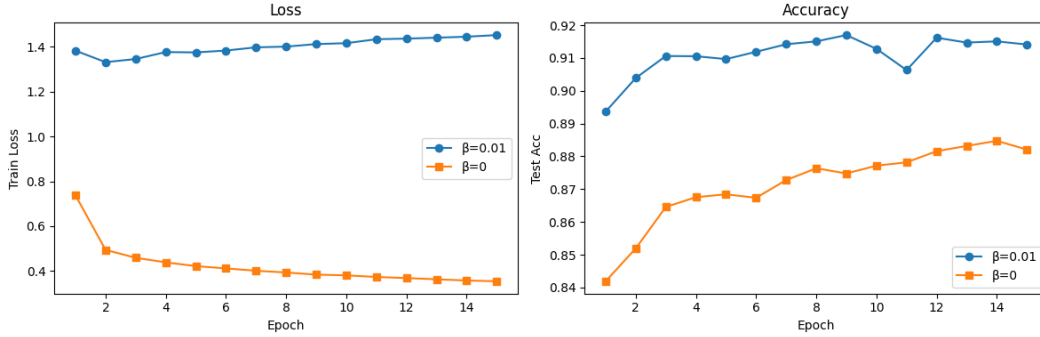


Figure 6: Test accuracy per epoch comparing models with and without SLQ-KL regularization. Regularization ($\beta = 0.01$) improves generalization accuracy.

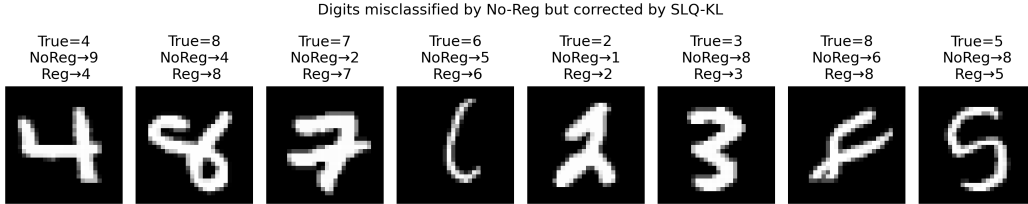


Figure 7: MNIST test examples where the SLQ-KL regularized model (Reg) correctly classifies digits that the unregularized model (NoReg) misclassifies. Top: true labels. Bottom: predicted labels for NoReg and Reg.

4 Conclusion

We introduced BOLT, a block-orthonormal SLQ method, and Subblock SLQ, a trace estimator tailored for memory-limited settings with partial matrix access. Both reformulate KL divergence as a trace computation and offer scalable alternatives to classical estimators. BOLT matches Hutch++ in complexity but has a simpler implementation and avoids spectral decay assumptions, improving performance in flat-spectrum regimes. Subblock SLQ operates on small submatrices, making it ideal for large-scale problems with strict memory constraints. The same framework also supports Wasserstein-2 (W_2) distance estimation, which avoids matrix inversion and remains valid for positive semidefinite covariances.

This family of estimators is broadly applicable across covariance estimation [32], stochastic trace estimation [15, 36, 23, 12], and large-scale scientific computing [4], where efficient KL evaluation is critical and full matrix access is often impractical. To our knowledge, this is the first unified KL framework based on trace functionals that handles full-rank, low-rank, and sparse regimes.

References

- [1] Moloud Abdar, Farhad Pourpanah, Sadiq Hussain, Dana Rezazadegan, Li Liu, Mohammad Ghavamzadeh, Paul Fieguth, Xiaochun Cao, Abbas Khosravi, U Rajendra Acharya, et al. A review of uncertainty quantification in deep learning: Techniques, applications and challenges. *Information fusion*, 76:243–297, 2021.
- [2] Sanjeev Arora, Yingyu Liang, and Tengyu Ma. A simple but tough-to-beat baseline for sentence embeddings. In *International Conference on Learning Representations*, 2017.
- [3] Haim Avron and Sivan Toledo. Randomized algorithms for estimating the trace of an implicit symmetric positive semidefinite matrix. *Journal of the ACM*, 58(2):8, 2011.
- [4] Zhaojun Bai, Gark Fahey, and Gene Golub. Some large-scale matrix computation problems. *Journal of Computational and Applied Mathematics*, 74(1-2):71–89, 1996.
- [5] Christos Boutsidis, Petros Drineas, Prabhajan Kambadur, Eugenia-Maria Kontopoulou, and Anastasios Zouzias. A randomized algorithm for approximating the log determinant of a symmetric positive definite matrix. *Linear Algebra and its Applications*, 533:95–117, 2017.
- [6] T Tony Cai, Tengyuan Liang, and Harrison H Zhou. Law of log determinant of sample covariance matrix and optimal estimation of differential entropy for high-dimensional gaussian distributions. *Journal of Multivariate Analysis*, 137:161–172, 2015.
- [7] Xingyu Cai, Jiayi Huang, Yuchen Bian, and Kenneth Church. Isotropy in the contextual embedding space: Clusters and manifolds. In *International Conference on Learning Representations*, 2021.
- [8] Michaël Defferrard, Xavier Bresson, and Pierre Vandergheynst. Convolutional neural networks on graphs with fast localized spectral filtering. *Advances in neural information processing systems*, 29, 2016.
- [9] Li Deng. The mnist database of handwritten digit images for machine learning research. *IEEE Signal Processing Magazine*, 29(6):141–142, 2012.
- [10] Kun Dong, David Eriksson, Hannes Nickisch, David Bindel, and Andrew Gordon Wilson. Scalable log determinants for gaussian process kernel learning. In *Advances in Neural Information Processing Systems*, pages 6327–6337, 2017.
- [11] Alan Edelman. Eigenvalues and condition numbers of random matrices. *SIAM journal on matrix analysis and applications*, 9(4):543–560, 1988.
- [12] Ethan N Epperly, Joel A Tropp, and Robert J Webber. Xtrace: Making the most of every sample in stochastic trace estimation. *SIAM Journal on Matrix Analysis and Applications*, 45(1):1–23, 2024.
- [13] J. Fan, Y. Fan, and J. Lv. High-dimensional covariance matrix estimation using a factor model. *Journal of Econometrics*, 147(1):186–197, 2008.
- [14] Jianqing Fan, Yuan Liao, and Martina Mincheva. High dimensional covariance matrix estimation in approximate factor models. *Annals of statistics*, 39(6):3320, 2011.
- [15] Rafael Díaz Fuentes, Marco Donatelli, Caterina Fenu, and Giorgio Mantica. Estimating the trace of matrix functions with application to complex networks. *Numerical Algorithms*, 92(1):503–522, 2023.
- [16] Reinhard Furrer and Thomas Bengtsson. Estimation of high-dimensional prior and posterior covariance matrices in kalman filter variants. *Journal of Multivariate Analysis*, 98(2):227–255, 2007.
- [17] San Gultekin and John Paisley. Nonlinear kalman filtering with divergence minimization. *IEEE Transactions on Signal Processing*, 65(23):6319–6331, 2017.
- [18] Insu Han, Dmitry Malioutov, Haim Avron, and Jinwoo Shin. Approximating spectral sums of large-scale matrices using stochastic chebyshev approximations. *SIAM Journal on Scientific Computing*, 39(4):A1558–A1585, 2017.
- [19] Michael F Hutchinson. A stochastic estimator of the trace of the influence matrix for laplacian smoothing splines. *Communications in Statistics-Simulation and Computation*, 18(3):1059–1076, 1989.

- [20] Elias Jarlebring, Jorge Sastre, and J Ibáñez. Polynomial approximations for the matrix logarithm with computation graphs. *Linear Algebra and its Applications*, 2024.
- [21] Shuli Jiang, Hai Pham, David P. Woodruff, and Qiuyi Zhang. Optimal sketching for trace estimation. In *Advances in Neural Information Processing Systems*, 2021.
- [22] Soheil Kolouri, Kimia Nadjahi, Umut Simsekli, Roland Badeau, and Gustavo Rohde. Generalized sliced wasserstein distances. *Advances in neural information processing systems*, 32, 2019.
- [23] Jacek Kuczyński and Henryk Woźniakowski. Estimating the largest eigenvalue by the power and lanczos algorithms with a random start. *SIAM journal on matrix analysis and applications*, 13(4):1094–1122, 1992.
- [24] O. Ledoit and M. Wolf. A well-conditioned estimator for large-dimensional covariance matrices. *Journal of Multivariate Analysis*, 88(2):365–411, 2004.
- [25] Lin Lin, Yousef Saad, and Chao Yang. Approximating spectral densities of large matrices. *SIAM review*, 58(1):34–65, 2016.
- [26] Karim Lounici. High-dimensional covariance matrix estimation with missing observations. *Bernoulli*, 20(3):1029–1058, 2014.
- [27] Raphael A Meyer, Cameron Musco, Christopher Musco, and David P Woodruff. Hutch++: Optimal stochastic trace estimation. In *Symposium on Simplicity in Algorithms (SOSA)*, pages 142–155. SIAM, 2021.
- [28] Jiaqi Mu and Pramod Viswanath. All-but-the-top: Simple and effective post-processing for word representations. In *International Conference on Learning Representations*, 2018.
- [29] Kimia Nadjahi, Alain Durmus, Lénaïc Chizat, Soheil Kolouri, Shahin Shahrampour, and Umut Simsekli. Statistical and topological properties of sliced probability divergences. *Advances in Neural Information Processing Systems*, 33:20802–20812, 2020.
- [30] Kimia Nadjahi, Alain Durmus, Pierre E. Jacob, Roland Badeau, and Umut Şimşekli. Fast approximation of the sliced-wasserstein distance using concentration of random projections. In *Advances in Neural Information Processing Systems*, 2021.
- [31] Khai Nguyen and Nhat Ho. Sliced wasserstein estimation with control variates. In *The Twelfth International Conference on Learning Representations*, 2024.
- [32] Florian Schäfer, Matthias Katzfuss, and Houman Owhadi. Sparse cholesky factorization by kullback–leibler minimization. *SIAM Journal on scientific computing*, 43(3):A2019–A2046, 2021.
- [33] Min-Jae Srivastava. Some tests concerning the covariance matrix in high-dimensional data. *Journal of the Japan Statistical Society*, 35(2):251–272, 2005.
- [34] Michael L Stein, Jie Chen, and Mihai Anitescu. Stochastic approximation of score functions for gaussian processes. *The Annals of Applied Statistics*, 2013.
- [35] Terence Tao and Van Vu. Random matrices: The distribution of the smallest singular values. *Geometric And Functional Analysis*, 20:260–297, 2010.
- [36] Shashanka Ubaru, Jie Chen, and Yousef Saad. Fast estimation of $\text{tr}(f(a))$ via stochastic lanczos quadrature. *SIAM Journal on Matrix Analysis and Applications*, 38(4):1075–1099, 2017.
- [37] Shashanka Ubaru and Yousef Saad. Applications of trace estimation techniques. In *International Conference on High Performance Computing in Science and Engineering*, pages 19–33. Springer, 2017.
- [38] Sheng Wang, Yuan Sun, Christopher Musco, and Zhifeng Bao. Public transport planning: When transit network connectivity meets commuting demand. In *Proceedings of the 2021 International Conference on Management of Data*, pages 1906–1919, 2021.
- [39] Jonathan Wenger, Geoff Pleiss, Philipp Hennig, John P. Cunningham, and Jacob R. Gardner. Preconditioning for scalable gaussian process hyperparameter optimization. In *Proceedings of the 39th International Conference on Machine Learning*, pages 23519–23547, 2022.
- [40] Kingsley Yeon. Deep univariate polynomial and conformal approximation. *arXiv preprint arXiv:2503.00698*, 2025.

- [41] Jennifer Zvonek, Andrew J Horning, and Alex Townsend. Conthutch++: Stochastic trace estimation for implicit integral operators. *SIAM Journal on Numerical Analysis*, 63(1):334–359, 2025.

A Proofs of Theoretical Results

A.1 Proof of Theorem 2.1

Proof. We first prove unbiasedness. Since the columns of V are orthonormal and drawn from the Haar measure on the Stiefel manifold, we have

$$\mathbb{E}[VV^T] = \frac{b}{n}I_n.$$

Therefore,

$$\mathbb{E}\left[\text{tr}(V^T f(A)V)\right] = \text{tr}\left(f(A) \mathbb{E}[VV^T]\right) = \frac{b}{n} \text{tr}(f(A)).$$

Defining

$$X(V) = \frac{n}{b} \text{tr}(V^T f(A)V),$$

it follows immediately that

$$\mathbb{E}[X(V)] = \text{tr}(f(A)).$$

In the extreme case $b = n$, any orthonormal V is orthogonal (i.e. $VV^T = I_n$) so that

$$\text{tr}(V^T f(A)V) = \text{tr}(f(A)),$$

and hence $X(V)$ is deterministic with zero variance.

Next, we derive the variance. Write the columns of V as v_1, v_2, \dots, v_b , so that

$$\text{tr}(V^T f(A)V) = \sum_{r=1}^b v_r^T f(A)v_r.$$

For a single scalar unit vector v uniformly distributed on the sphere in \mathbb{R}^n , we express v in the eigenbasis of A by writing $A = Q\Lambda Q^T$ with $\Lambda = \text{diag}(\lambda_1, \dots, \lambda_n)$ and $v = Qz$. Then,

$$v^T f(A)v = z^T f(\Lambda)z = \sum_{i=1}^n f(\lambda_i)z_i^2.$$

Because z is uniformly distributed on the unit sphere, the moments of its components are:

$$\mathbb{E}[z_i^2] = \frac{1}{n}, \quad \mathbb{E}[z_i^4] = \frac{3}{n(n+2)}, \quad \mathbb{E}[z_i^2 z_j^2] = \frac{1}{n(n+2)} \quad (i \neq j).$$

Thus,

$$\begin{aligned} \mathbb{E}\left[\left(v^T f(A)v\right)^2\right] &= \sum_{i=1}^n f(\lambda_i)^2 \mathbb{E}[z_i^4] + \sum_{i \neq j} f(\lambda_i)f(\lambda_j) \mathbb{E}[z_i^2 z_j^2] \\ &= \frac{3}{n(n+2)} \sum_{i=1}^n f(\lambda_i)^2 + \frac{1}{n(n+2)} \left[\left(\sum_{i=1}^n f(\lambda_i) \right)^2 - \sum_{i=1}^n f(\lambda_i)^2 \right] \\ &= \frac{2}{n(n+2)} \sum_{i=1}^n f(\lambda_i)^2 + \frac{1}{n(n+2)} \left(\sum_{i=1}^n f(\lambda_i) \right)^2. \end{aligned}$$

Therefore, the variance of a scalar quadratic form is

$$\begin{aligned} \text{Var}[v^T f(A)v] &= \mathbb{E}\left[\left(v^T f(A)v\right)^2\right] - \left(\frac{1}{n} \sum_{i=1}^n f(\lambda_i)\right)^2 \\ &= \frac{2}{n(n+2)} \sum_{i=1}^n f(\lambda_i)^2 - \frac{2}{n^2(n+2)} \left(\sum_{i=1}^n f(\lambda_i) \right)^2. \end{aligned}$$

Now, consider the block estimator. Define

$$S = \sum_{r=1}^b v_r^T f(A) v_r.$$

If the b vectors were independent, we would have

$$\text{Var}(S) = b \text{Var}[v^T f(A) v].$$

However, because the columns of V are orthonormal, for any $i \neq j$ we have

$$\text{Cov}\left(v_i^T f(A) v_i, v_j^T f(A) v_j\right) = -\frac{1}{n-1} \text{Var}\left(v^T f(A) v\right).$$

Thus,

$$\begin{aligned} \text{Var}(S) &= \sum_{r=1}^b \text{Var}[v^T f(A) v] + \sum_{r \neq s} \text{Cov}\left(v_r^T f(A) v_r, v_s^T f(A) v_s\right) \\ &= b \text{Var}[v^T f(A) v] - \frac{b(b-1)}{n-1} \text{Var}[v^T f(A) v] \\ &= \text{Var}[v^T f(A) v] \left(b - \frac{b(b-1)}{n-1}\right). \end{aligned}$$

We call this the *self-averaging effect*. Since

$$X(V) = \frac{n}{b} S,$$

we obtain

$$\text{Var}[X(V)] = \left(\frac{n}{b}\right)^2 \text{Var}(S) = \left(\frac{n}{b}\right)^2 \text{Var}[v^T f(A) v] \left(b - \frac{b(b-1)}{n-1}\right).$$

Substituting the expression for $\text{Var}[v^T f(A) v]$ yields

$$\text{Var}[X(V)] = \left(\frac{n}{b}\right)^2 \frac{2}{n(n+2)} \left(\sum_{i=1}^n f(\lambda_i)^2 - \frac{1}{n} (\text{tr}(f(A)))^2\right) \left(b - \frac{b(b-1)}{n-1}\right).$$

Simplifying, we note that

$$\left(\frac{n}{b}\right)^2 \frac{2}{n(n+2)} = \frac{2n}{b^2(n+2)}.$$

Thus,

$$\text{Var}[X(V)] = \frac{2n}{b^2(n+2)} \left(b - \frac{b(b-1)}{n-1}\right) \left(\sum_{i=1}^n f(\lambda_i)^2 - \frac{1}{n} (\text{tr}(f(A)))^2\right).$$

We can factor a b from the term in parentheses:

$$b - \frac{b(b-1)}{n-1} = b \left(1 - \frac{b-1}{n-1}\right),$$

so that

$$\text{Var}[X(V)] = \frac{2n}{b^2(n+2)} b \left(1 - \frac{b-1}{n-1}\right) \left(\sum_{i=1}^n f(\lambda_i)^2 - \frac{1}{n} (\text{tr}(f(A)))^2\right).$$

Cancel one b to obtain

$$\text{Var}[X(V)] = \frac{2n}{b(n+2)} \left(1 - \frac{b-1}{n-1}\right) \left(\sum_{i=1}^n f(\lambda_i)^2 - \frac{1}{n} (\text{tr}(f(A)))^2\right).$$

Where,

$$\frac{2n}{b(n+2)} \left(1 - \frac{b-1}{n-1}\right) = -\frac{2n}{(n+2)(n-1)} + \frac{2n^2}{(n+2)(n-1)} \frac{1}{b} + 0 \cdot \frac{1}{b^2} + \mathcal{O}(b^{-3}) = \mathcal{O}(b^{-1})$$

Averaging over q independent probes gives

$$\text{Var}[\hat{T}] = \frac{1}{q} \text{Var}[X(V)].$$

Therefore the variance decays like $\mathcal{O}(\frac{1}{qb})$.

Finally, since each $X(V)$ is almost surely contained in $[\ell_{\min}, \ell_{\max}]$, Hoeffding's inequality implies that for any $\varepsilon > 0$

$$\mathbb{P}\left(\left|\hat{T} - \text{tr}(f(A))\right| \geq \varepsilon\right) \leq 2 \exp\left(-\frac{2q \varepsilon^2}{(\ell_{\max} - \ell_{\min})^2}\right).$$

Equivalently, with probability at least $1 - \delta$,

$$\left|\hat{T} - \text{tr}(f(A))\right| \leq (\ell_{\max} - \ell_{\min}) \sqrt{\frac{\ln(2/\delta)}{2q}}.$$

□

A.2 Proof of Lemma 2.2

Proof. We begin by diagonalizing B . Since B is symmetric, write

$$B = Q \text{diag}(f(\lambda_1), \dots, f(\lambda_n)) Q^T,$$

and set $\tilde{V} = Q^T V$. Then $\tilde{V} \in \mathbb{R}^{n \times b}$ still satisfies $\tilde{V}^T \tilde{V} = I_b$, and

$$\text{tr}(V^T B V) = \text{tr}(\tilde{V}^T \text{diag}(f(\lambda_i)) \tilde{V}) = \sum_{i=1}^n f(\lambda_i) \tilde{V}_{i,*} \cdot \tilde{V}_{i,*}^T = \sum_{i=1}^n f(\lambda_i) P_{ii},$$

where $P = \tilde{V} \tilde{V}^T$ is an orthogonal projector of rank b . Hence

$$\hat{T}_{\text{block}} = \frac{n}{b} \sum_{i=1}^n f(\lambda_i) P_{ii}.$$

Define the weights $\alpha_i = P_{ii}/b$. Since $\sum_i P_{ii} = \text{tr}(P) = b$, it follows that

$$\sum_{i=1}^n \alpha_i = 1 \quad \text{and} \quad \sum_{i=1}^n \left(\alpha_i - \frac{1}{n}\right) = 0.$$

Writing $\delta_i = \alpha_i - \frac{1}{n}$, we obtain

$$\hat{T}_{\text{block}} - T = n \sum_{i=1}^n \delta_i f(\lambda_i).$$

Because the δ_i sum to zero, the maximal shift in weighted average from the smallest to the largest eigenvalue gives

$$|\hat{T}_{\text{block}} - T| \leq n (\max_i f(\lambda_i) - \min_i f(\lambda_i)) \max_i |\delta_i|.$$

Noting that $0 \leq P_{ii} \leq 1$ implies $0 \leq \alpha_i \leq 1/b$, and since $1/n \leq 1/b$, we have $\max_i |\delta_i| \leq 1/b$. Therefore

$$|\hat{T}_{\text{block}} - T| \leq \frac{n}{b} (\max_i f(\lambda_i) - \min_i f(\lambda_i)).$$

Set

$$\Delta_{\text{scalar}} = n (\max_i f(\lambda_i) - \min_i f(\lambda_i)), \quad C_0 = \frac{\Delta_{\text{scalar}}}{T},$$

so that algebraically

$$\Delta_{\text{scalar}} = C_0 T, \quad \Delta_{\text{block}} = \frac{\Delta_{\text{scalar}}}{b} = \frac{C_0 T}{b}.$$

Thus every single block probe lies in an interval of length Δ_{block} . Similarly, each normalized Rademacher probe $v^T B v$ lies in an interval of length Δ_{scalar} .

We now apply Hoeffding's inequality. If X_1, \dots, X_q are i.i.d. in an interval of length Δ , then

$$\Pr\left(\left|\frac{1}{q} \sum_{k=1}^q X_k - \mathbb{E}[X_1]\right| \geq t\right) \leq 2 \exp\left(-\frac{2q t^2}{\Delta^2}\right).$$

1. Block SLQ: one probe ($q = 1$) of length $\Delta_{\text{block}} = C_0 T/b$. Since $b = \lfloor N_{\text{mv}}/2 \rfloor$, deterministically

$$|\hat{T}_{\text{block}} - T| \leq \Delta_{\text{block}} = O\left(\frac{1}{b}\right) = O\left(\frac{1}{N_{\text{mv}}}\right),$$

i.e. $O(N_{\text{mv}}^{-1})$ error with probability 1.

2. Scalar SLQ: $q = \lfloor N_{\text{mv}}/2 \rfloor$ probes each of length $\Delta_{\text{scalar}} = C_0 T$. Hoeffding gives, with probability $\geq 1 - \delta$,

$$|\hat{T}_{\text{scalar}} - T| \leq \Delta_{\text{scalar}} \sqrt{\frac{\ln(2/\delta)}{2q}} = O\left(q^{-1/2}\right) = O\left(N_{\text{mv}}^{-1/2}\right).$$

Combining these two cases completes the proof of the $O(N_{\text{mv}}^{-1})$ versus $O(N_{\text{mv}}^{-1/2})$ high-probability error-decay rates.

For the asymptotic high-probability bound, we write

$$V \in \mathbb{R}^{n \times n}, \quad V^T V = I_n,$$

where V is drawn uniformly from the Stiefel manifold $\text{St}(n, n)$, i.e., the space of orthogonal $n \times n$ matrices. Define the rotated probe

$$\tilde{V} = Q^T V = [\tilde{V}_1 \mid \tilde{V}_2],$$

with $\tilde{V}_1 \in \mathbb{R}^{n \times b}$, and observe that

$$\tilde{V}^T D \tilde{V} \stackrel{\text{dist}}{=} V^T B V,$$

by rotational invariance. The true trace is then

$$T = \text{tr}(\tilde{V}^T D \tilde{V}) = \sum_{i=1}^n D_i.$$

Introduce the selector matrix

$$P_s = \begin{bmatrix} I_b \\ 0_{(n-b) \times b} \end{bmatrix} \in \mathbb{R}^{n \times b},$$

so that

$$P_s^T \tilde{V}^T D \tilde{V} P_s = \tilde{V}_1^T D \tilde{V}_1.$$

By Lemma 3.4 (subblock Wishart sampling with $m = b$ and covariance $\Sigma = P_s^T D P_s = \text{diag}(D_1, \dots, D_b)$), the $b \times b$ matrix $\tilde{V}_1^T D \tilde{V}_1 \sim W_b(\text{diag}(D_1, \dots, D_b), b)$. Hence its trace admits the chi-square expansion

$$\text{tr}(\tilde{V}_1^T D \tilde{V}_1) = \sum_{i=1}^b D_i \chi_i^2, \quad \chi_i^2 \sim \chi_1^2 \text{ indep.}$$

Thus the block-SLQ estimator is

$$\hat{T}_{\text{block}} = \frac{n}{b} \text{tr}(\tilde{V}_1^T D \tilde{V}_1) = \frac{n}{b} \sum_{i=1}^b D_i \chi_i^2,$$

and

$$\widehat{T}_{\text{block}} - T = \frac{n}{b} \sum_{i=1}^b D_i \chi_i^2 - \sum_{i=1}^n D_i.$$

Let

$$\bar{D} = \frac{1}{b} \sum_{j=1}^b D_j, \quad \delta_i = D_i - \bar{D},$$

so that under the mild assumption $\delta_i = O(1/n)$ for $1 \leq i \leq b$,

$$\frac{n}{b} \sum_{i=1}^b D_i - \sum_{i=1}^n D_i = n\bar{D} - \sum_{i=1}^n D_i = O(\frac{1}{b}).$$

Moreover,

$$\frac{n}{b} \sum_{i=1}^b D_i \chi_i^2 - \frac{n}{b} \sum_{i=1}^b D_i = \frac{n}{b} \sum_{i=1}^b D_i (\chi_i^2 - 1) = \frac{n}{b} \sum_{i=1}^b (\chi_i^2 - 1) (\bar{D} + \delta_i).$$

The \bar{D} -term cancels up to $O(1/b)$, leaving

$$\widehat{T}_{\text{block}} - T = \frac{n}{b} \sum_{i=1}^b (\chi_i^2 - 1) \delta_i + O(\frac{1}{b}).$$

Set

$$X_i = (\chi_i^2 - 1) \delta_i, \quad Y_i = \frac{n}{b} X_i,$$

so that $\mathbb{E}[X_i] = 0$ and $\text{Var}(X_i) = 2\delta_i^2$. Hence

$$\sigma^2 = \sum_{i=1}^b \text{Var}(Y_i) = 2 \left(\frac{n}{b}\right)^2 \sum_{i=1}^b \delta_i^2 = O(\frac{1}{b}).$$

Define

$$S = \sum_{i=1}^b Y_i, \quad Y_i = \frac{n}{b} \delta_i (\chi_i^2 - 1), \quad \delta_i = \tilde{D}_i - \frac{1}{b} \sum_{j=1}^b \tilde{D}_j, \quad (\text{A.1})$$

so $\mathbb{E}[S] = 0$. Since each $\chi_i^2 - 1$ is sub-exponential with $\|\chi_i^2 - 1\|_{\psi_1} \leq 4$ and $|\delta_i| = O(1/n)$, the sub-exponential norm satisfies

$$\|Y_i\|_{\psi_1} = \frac{n}{b} |\delta_i| \|\chi_i^2 - 1\|_{\psi_1} = O(\frac{1}{b}).$$

Set

$$\beta = \max_i \|Y_i\|_{\psi_1} = O(\frac{1}{b}).$$

By the Bernstein mgf condition, for $|\lambda| < \beta^{-1}$,

$$\mathbb{E} \exp(\lambda Y_i) \leq \exp\left(\frac{\lambda^2 \sigma^2}{2(1 - \beta|\lambda|)}\right),$$

which yields the tail bound, for all $t > 0$,

$$\Pr(|S| \geq t) \leq 2 \exp\left(-\frac{t^2}{2(\sigma^2 + \beta t)}\right). \quad (\text{A.2})$$

Take

$$t = c \sigma^2 = c \left(\frac{n}{b}\right)^2 \sum_{i=1}^b \delta_i^2 = O(\frac{1}{b}),$$

and note $\beta t = O(b^{-2}) \ll \sigma^2 = O(b^{-1})$. Therefore

$$\sigma^2 + \beta t = \sigma^2(1 + O(b^{-1})),$$

and substitution into (A.2) gives

$$-\frac{t^2}{2(\sigma^2 + \beta t)} = -\frac{c^2 \sigma^4}{2(\sigma^2 + \beta t)} = -\frac{c^2 \sigma^2}{2}(1 + O(b^{-1})) = -\frac{c^2 C}{2b}(1 + O(b^{-1})),$$

where $C = 2 \sum_i \delta_i^2 = O(1)$. Hence $\Pr(|S| \geq t) \leq 2 \exp(-\Omega(b))$, so $S = O_p(1/b)$. Combining with $|\Delta| = O(1/b)$ yields

$$\widehat{T}_{\text{block}} - T = S + \Delta = O_p\left(\frac{1}{b}\right),$$

and since $N_{\text{mv}} = 2b$ this is equivalent to $|\widehat{T}_{\text{block}} - T| = O(N_{\text{mv}}^{-1})$, as claimed. \square

A.3 Proof of Lemma 3.4

Proof. Let $P_S \in \{0, 1\}^{n \times s}$ be the coordinate-selection matrix that extracts the s indices in S . For each Gaussian sample $u_i \sim \mathcal{N}(0, \Sigma)$, the projected vector

$$v_i = P_S^T u_i$$

is an s -dimensional Gaussian. Its mean is $\mathbb{E}[v_i] = P_S^T \mathbb{E}[u_i] = 0$, and its covariance is

$$\mathbb{E}[v_i v_i^T] = P_S^T \mathbb{E}[u_i u_i^T] P_S = P_S^T \Sigma P_S.$$

Hence

$$v_1, \dots, v_m \sim \text{iid } \mathcal{N}(0, P_S^T \Sigma P_S).$$

By definition, the unnormalized sample covariance of these projections is

$$\widetilde{\Sigma}_S = \sum_{i=1}^m v_i v_i^T = \sum_{i=1}^m (P_S^T u_i)(P_S^T u_i)^T = P_S^T \left(\sum_{i=1}^m u_i u_i^T \right) P_S = P_S^T \widetilde{\Sigma} P_S,$$

which is a central Wishart matrix $W_s(P_S^T \Sigma P_S, m)$.

A key property of the Wishart distribution is that if the degrees of freedom m satisfy $m \geq s$ and the scale matrix $P_S^T \Sigma P_S$ is full rank (which it is, since $\Sigma \succ 0$), then $\widetilde{\Sigma}_S$ is invertible with probability one. Equivalently,

$$\Pr(\det \widetilde{\Sigma}_S = 0) = 0,$$

so $\text{rank}(\widetilde{\Sigma}_S) = s$ almost surely. Conversely, if $m < s$, then $\widetilde{\Sigma}_S$ has rank at most m , and so the transition from full-rank to singular behavior occurs precisely at $s = m$. \square

A.4 Proof of Lemma 3.1

Proof. Consider the full index set $I = \{1, 2, \dots, n\}$, and suppose that in a single sampling of a subblock, a subset $S \subset I$ of size s is chosen uniformly at random. For any fixed index $i \in I$, the probability that i is included in S is exactly $\frac{s}{n}$ since the block is selected uniformly without replacement; hence, the probability that index i does not appear in a single subblock is $1 - \frac{s}{n}$. Because the t subblocks are drawn independently, the probability that index i is not covered in any of the t subblocks is given by $\left(1 - \frac{s}{n}\right)^t$. In order to guarantee that every index in I appears in at least one subblock, one must control the probability that there exists at least one index that is never sampled. Applying the union bound over all n indices, we find that the probability that at least one index is omitted in all t draws is bounded above by

$$n \left(1 - \frac{s}{n}\right)^t.$$

In order for the union of the subblocks to equal I with probability at least $1 - \varepsilon$, it suffices to require that

$$n \left(1 - \frac{s}{n}\right)^t \leq \varepsilon.$$

Taking natural logarithms on both sides, we obtain

$$\log n + t \log\left(1 - \frac{s}{n}\right) \leq \log \varepsilon.$$

Since for any x with $0 < x < 1$ it holds that $\log(1 - x) \leq -x$, by setting $x = \frac{s}{n}$ we have $\log\left(1 - \frac{s}{n}\right) \leq -\frac{s}{n}$. Therefore, the inequality above is further bounded by

$$\log n - t \frac{s}{n} \leq \log \varepsilon.$$

Rearranging the terms yields

$$t \frac{s}{n} \geq \log n - \log \varepsilon,$$

or equivalently,

$$t \geq \frac{n}{s} (\log n - \log \varepsilon) = \frac{n}{s} \log\left(\frac{n}{\varepsilon}\right).$$

Thus, if the number of subblocks t satisfies

$$t \geq \frac{n}{s} \log\left(\frac{n}{\varepsilon}\right),$$

then the probability that the union of the indices from these t subblocks equals the full set $\{1, 2, \dots, n\}$ is at least $1 - \varepsilon$. This completes the proof. \square

A.5 Proof of Lemma 3.2

Proof. First, for any $i \in \{1, \dots, n\}$, $\Pr(i \in S) = s/n$, so

$$\mathbb{E}[\text{tr}(f(A)_S)] = \sum_{i=1}^n \Pr(i \in S) f(A)_{ii} = \frac{s}{n} \text{tr}(f(A)),$$

and hence $\mathbb{E}[X(S)] = \text{tr}(f(A))$.

Next, since $f(A) \succeq 0$ and f is nondecreasing, for the coordinate projector P_S we have the Loewner ordering

$$P_S f(A) P_S \preceq f(A).$$

Taking traces—which preserves semidefinite inequalities—gives $\text{tr}(f(A)_S) = \text{tr}(P_S f(A) P_S) \leq \text{tr}(f(A))$, so each block-trace is a lower bound.

Finally, by Full Coverage via Block Sampling, if $t \geq \frac{n}{s} \log(n/\varepsilon)$, then with probability $1 - \varepsilon$ the union U of the S_i equals $\{1, \dots, n\}$. For the corresponding projector $P_U = I$, we have

$$P_U f(A) P_U = f(A) \implies \text{tr}(f(A)_U) = \text{tr}(f(A)),$$

completing the proof. \square

A.6 Proof of Theorem 3.3

Proof. Write the Chebyshev expansion

$$p_m(A) = \sum_{k=0}^m c_k A^k.$$

We will show that for each $0 \leq k \leq m$ and every $i, j \in S$,

$$[A^k]_{ij} = [(A_{S_r, S_r})^k]_{ij}.$$

Indeed, by the definition of matrix powers,

$$[A^k]_{ij} = \sum_{t_1, \dots, t_{k-1}=1}^n A_{i, t_1} A_{t_1, t_2} \cdots A_{t_{k-1}, j}.$$

Each nonzero term in this sum corresponds to a walk of length k in G from i to j through vertices t_1, \dots, t_{k-1} . Since $i \in S$ and $k \leq r$, every intermediate vertex and the endpoint j lie within distance

$\leq k \leq r$ of S , hence belong to S_r . Thus all indices in any nonzero product lie in S_r , and we may restrict each summation to $t_\ell \in S_r$. But that restricted sum is exactly the (i, j) -entry of $(A_{S_r, S_r})^k$. Therefore

$$[A^k]_{ij} = [(A_{S_r, S_r})^k]_{ij},$$

as claimed.

Summing these equalities over $k = 0, \dots, m$ with weights c_k gives

$$[p_m(A)]_{S, S} = \sum_{k=0}^m c_k [A^k]_{S, S} = \sum_{k=0}^m c_k [(A_{S_r, S_r})^k]_{S, S} = [p_m(A_{S_r, S_r})]_{S, S}.$$

Finally, since ${}^\circ p_m \leq r$, no walk of length $\leq m \leq r$ can leave S once it has returned; restricting further from the S_r -block to the S -block recovers $[p_m(A_{S_r, S_r})]_{S, S} = p_m(A_S)$.

To bound Δ_S , insert and subtract p_m twice:

$$\Delta_S = [\text{tr}(f(A)_S) - \text{tr}(p_m(A)_S)] + [\text{tr}(p_m(A)_S) - \text{tr}(p_m(A_S))] + [\text{tr}(p_m(A_S)) - \text{tr}(f(A_S))].$$

The middle term vanishes by the block-wise equality just shown. Meanwhile the uniform approximation $\|f - p_m\|_\infty \leq \varepsilon$ implies $\|f(A) - p_m(A)\|_2 \leq \varepsilon$ and similarly on the submatrix. Hence each of the two endpoint differences in trace is bounded by $s\varepsilon$, giving $|\Delta_S| \leq s\varepsilon + 0 + s\varepsilon = 2s\varepsilon$. \square

B FLOPS count of various matrix trace estimator

The first three estimators, XTrace, XNysTrace [12], and Hutch++, all build on the idea of combining low-rank sketching with randomized probing, but differ in how they form the sketch and treat the residual. These structural differences directly influence the computational cost of each method, as summarized in Table 2.

Table 2: Flop counts to achieve ε -accuracy ($m, b \sim \Theta(\varepsilon^{-1})$) (Naïve).

Method	# Mat-vecs	Overhead (post-mat-vec)	Total flops
XTrace (Naïve)	m	$O(Nm^3 + m^4 + Nm^2)$	$O(N^2m + Nm^3 + m^4 + Nm^2)$
XNysTrace (Naïve)	m	$O(m^4 + Nm)$	$O(N^2m + m^4 + Nm)$
Hutch++	m	$O(Nm^2)$	$O(N^2m + Nm^2)$
BOLT	m	$O(Nm^2)$	$O(N^2m + Nm^2)$

XTrace enforces the exchangeability principle by constructing a leave-one-out low-rank approximation for each of the $m/2$ probing directions. It draws $\omega_1, \dots, \omega_{m/2}$ and forms the sketch matrix $Y = A[\omega_1 \cdots \omega_{m/2}] \in \mathbb{R}^{N \times (m/2)}$. For each i , the i th column is removed to obtain Y_{-i} , and an orthonormal basis $Q^{(i)} = \text{orth}(Y_{-i})$ is computed. The trace estimator is

$$\hat{t}_i = \text{tr}(Q^{(i)T} A Q^{(i)}) + \omega_i^T (I - Q^{(i)} Q^{(i)T}) A (I - Q^{(i)} Q^{(i)T}) \omega_i,$$

and the final output is $\widehat{\text{tr}}(A) = \frac{2}{m} \sum_{i=1}^{m/2} \hat{t}_i$. Computing all QR factorizations costs $O(Nm^3)$, pseudoinverses contribute $O(m^4)$, and the trace and residual evaluations require $O(Nm^2)$.

XNysTrace modifies this by using Nyström approximations. It constructs

$$A\langle\Omega_{-i}\rangle = A\Omega_{-i} (\Omega_{-i}^T A \Omega_{-i})^\dagger (\Omega_{-i}^T A)^T, \quad \hat{t}_i = \text{tr}(A\langle\Omega_{-i}\rangle) + \omega_i^T (A - A\langle\Omega_{-i}\rangle) \omega_i,$$

requiring an SVD or Cholesky on each $(m-1) \times (m-1)$ matrix, yielding $O(m^4)$ total overhead. The rest of the cost mirrors that of XTrace.

Efficient Implementation via Rank-One Update. In Section 2.1 of [12], a more efficient implementation of the XTrace estimator is developed. Let $A \in \mathbb{R}^{N \times N}$ and define the test matrix $\Omega = [\omega_1 \cdots \omega_{m/2}] \in \mathbb{R}^{N \times (m/2)}$. One first forms the sketch $Y = A\Omega$ and performs the QR decomposition $Y = QR$. Then, following the analysis in Appendix A.2 of [12], the leave-one-out orthogonal projectors are computed by

$$Q^{(i)} Q^{(i)T} = Q(I - s_i s_i^T) Q^T,$$

where each $s_i \in \mathbb{R}^m$ is a unit vector in the nullspace of R_{-i}^T . All vectors $s_1, \dots, s_{m/2}$ can be constructed simultaneously via

$$S = R^{-*} D,$$

where D is a diagonal matrix used to normalize the columns of S . This reduces the cost of all leave-one-out projectors to $O(m^3)$ total.

Hutch++. Hutch++ achieves variance reduction without leave-one-out constructions by splitting the total of m mat-vecs into three groups of size $s = m/3$. The first s probes are used to build a low-rank sketch $Y = A[\omega_{s+1}, \dots, \omega_{2s}]$, and an orthonormal basis $Q = \text{orth}(Y)$ is computed. This basis is then used to exactly compute the projected trace $\text{tr}(Q^T A Q)$. The remaining s probes are used to estimate the residual trace $\text{tr}((I - Q Q^T) A (I - Q Q^T))$ via a Hutchinson-type average. The QR factorization of the $N \times s$ matrix Y costs $O(N s^2) = O(N m^2)$, and the subsequent evaluation of both the projected trace and residual adds another $O(N m^2)$, since each involves applying A and performing inner products with matrices of size $N \times s$. The total mat-vec cost is again $O(N^2 m)$, as A is applied to all m probe vectors. Therefore, the total cost is $O(N^2 m + N m^2)$, significantly lower than the leave-one-out variants due to the reuse of the same sketching basis across all evaluations.

While all methods share a leading matrix-vector cost of $O(N^2 m)$, XTrace and XNysTrace incur an additional $O(m^3)$ overhead from the rank-one update implementation [12]. These extra costs make Hutch++ and BOLT more scalable, especially in settings where subblock extensions or memory constraints are relevant. A summary of the computational complexity under this optimized implementation is provided in Table 1.

C Eigenvalue Distributions for Wishart Matrices

We summarize key results about the eigenvalue distribution of Wishart matrices, which explain the rank transition behavior discussed in the main text.

Let $\tilde{\Sigma} = \sum_{i=1}^m u_i u_i^T$, where $u_i \sim \mathcal{N}(0, \Sigma)$ and $\Sigma \in \mathbb{R}^{n \times n}$ is full rank. Then $\tilde{\Sigma} \sim W_n(\Sigma, m)$ is a sample covariance matrix of rank at most m . For any index set $S \subset \{1, \dots, n\}$ of size s , the subblock $\tilde{\Sigma}_S = P_S^T \tilde{\Sigma} P_S \sim W_s(P_S^T \Sigma P_S, m)$ is itself Wishart-distributed. The smallest eigenvalue of $\tilde{\Sigma}_S$ undergoes a sharp phase transition at $s = m$: subblocks are full rank almost surely for $s \leq m$, while for $s > m$, they become singular with probability one. This transition governs when subblock-based KL estimation remains well-posed.

We recall the following classical result:

Theorem C.1 (Smallest Eigenvalue Distribution for Wishart Matrices with Gaussian Entries (Theorem 4.3, [11])). *Let $W(m, n)$ be a Wishart matrix, formed from an $m \times n$ matrix with independent, mean-zero Gaussian entries. Then the probability density function (pdf) of the smallest eigenvalue λ_{\min} is given by*

$$f(\lambda) = c_{m,n} \lambda^{\frac{n-m-1}{2}} e^{-\lambda/2} g(\lambda),$$

where

$$g(\lambda) = \begin{cases} P_{m,n}(\lambda), & \text{if } n - m \text{ is odd,} \\ Q_{m,n}(\lambda) U\left(\frac{m-1}{2}, \frac{1}{2}, \lambda\right) + R_{m,n}(\lambda) U'\left(\frac{m-1}{2}, \frac{1}{2}, \lambda\right), & \text{if } n - m \text{ is even.} \end{cases}$$

Here, $U(a, b, \lambda)$ denotes the Tricomi confluent hypergeometric function, and U' its derivative with respect to λ . The constant $c_{m,n}$ depends explicitly on m and n and products of Gamma functions.

Remark C.1. Although Theorem C.1 assumes Gaussian entries, similar eigenvalue statistics hold for a broad class of random matrices satisfying finite-moment assumptions, by universality results such as those of Tao and Vu [35].

In the special case where $W(m, m)$ is a square Wishart matrix and $m \rightarrow \infty$, the scaled smallest eigenvalue $m \lambda_{\min}$ converges in distribution to a density

$$f(x) = \frac{1 + \sqrt{x}}{2\sqrt{x}} e^{-(x/2 + \sqrt{x})}.$$

Figure 8 shows the histogram of scaled smallest eigenvalues for $m = 50$, while Figures 9–10 illustrate the transition from full-rank to singular subblocks as s exceeds m .

D Numerical Experiment Details

Synthetic Cholesky Estimation. We generate a covariance matrix Σ using a Gaussian kernel with bandwidth $\sigma = 2.0$ and simulate m samples from $\mathcal{N}(0, \Sigma)$. For the full-rank case, we use $m = 10000$, and for the singular case, $m = 50$. Let $Y \in \mathbb{R}^{m \times n}$ denote the matrix of samples. We estimate the Cholesky factor L by solving for $P = LL^T$ such that $P\Sigma \approx I$, using Newton’s method on each column. When $m < n$, the estimate becomes low-rank, and standard KL divergence becomes undefined.

To compute the proxy KL divergence, we apply the unified block SLQ estimator. This computes $\frac{1}{2} \text{tr}(f(L^T \Sigma L))$ by sampling subblocks of size $s \times s$ from the effective dimension of L , performing block Lanczos iterations, and averaging the spectral quadrature estimates. In the full-rank case, we compare this estimate against the direct KL divergence. In the singular case, only the SLQ estimate is computable. Figure 12 shows the KL divergence estimates under the least-squares Cholesky solution for full-rank and singular settings. Figure 13 shows the same comparison when using a sparse Cholesky solver, where the singular-case KL is significantly reduced.

MNIST Classification with SLQ-KL Regularization. We train a simple multilayer perceptron (MLP) on MNIST with an architecture consisting of a fully connected input layer (784 to 8), a ReLU activation, and a final linear layer projecting to 10 output classes. The model is trained on 10% of the MNIST dataset and evaluated on the remaining 90%.

We use a mini-batch size of 4 and apply the SLQ-KL penalty to the hidden activations of the first layer. At each training step, we compute the hidden activation matrix $H \in \mathbb{R}^{4 \times 8}$, center it to obtain H_c , and compute the empirical covariance matrix

$$\Sigma = \frac{1}{3} H_c^T H_c \in \mathbb{R}^{8 \times 8}.$$

To estimate the KL penalty $\frac{1}{2} \text{tr}(f(\Sigma))$, we apply the unified block SLQ estimator with

$$s = \min(\text{rank}(\Sigma), \text{hidden_dim}), \quad t = 3,$$

subblocks, using $q = 2$ orthonormal block probes and $k = 8$ Lanczos steps per subblock. The identity matrix $L = I$ is used as the Cholesky factor. This estimate is added to the cross-entropy loss with weight $\beta = 0.01$. The network is optimized using Adam with learning rate 10^{-3} for 15 epochs. We compare the regularized model against a baseline trained with $\beta = 0$, holding all other parameters fixed.

Figures 6 and 7 report the training curves and final test-time predictions. KL-regularized training improves generalization and corrects several classification errors made by the unregularized model.

E Supplementary Figures

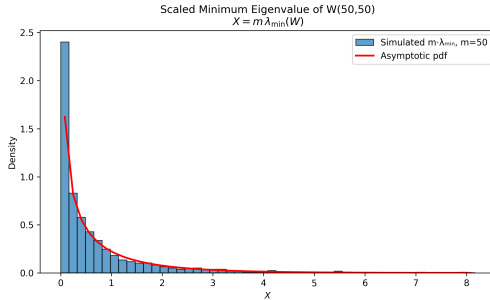


Figure 8: Histogram of scaled smallest eigenvalue of $W(m, m)$ for $m = 50$.

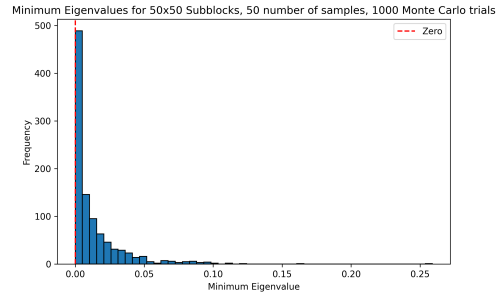


Figure 9: Histogram of smallest eigenvalue of A_s when $s = m$.

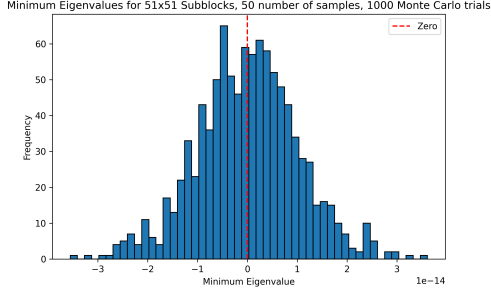


Figure 10: Histogram of the smallest eigenvalue of A_s when $s > m$.

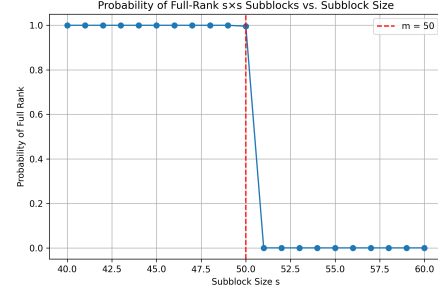


Figure 11: Histogram of the smallest eigenvalue of A_s when $s = m$.

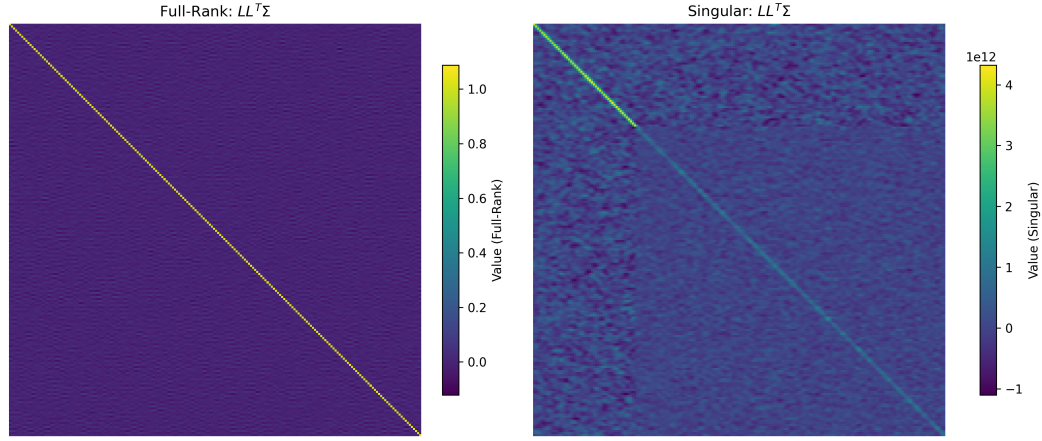


Figure 12: Full-Rank KL: 1.05
Singular Case KL: 1.07e+14

F Algorithms

F.1 Stochastic Lanczos Quadrature (SLQ)

Algorithm 3 Stochastic Lanczos Quadrature (SLQ) Estimator for the KL Divergence

- 1: **Input:** Covariance operator Σ , Cholesky factor L , number of probes q , Lanczos steps k .
 - 2: Define $\mathcal{A}(v) = L^T[\Sigma(Lv)]$.
 - 3: **for** $i = 1, \dots, q$ **do**
 - 4: Generate $z_i \in \{-1, 1\}^n$, normalize $v_i = z_i / \|z_i\|$.
 - 5: Run Lanczos with \mathcal{A} starting from v_i , obtain tridiagonal T_i .
 - 6: Diagonalize $T_i = U_i \text{diag}(\mu_{i1}, \dots, \mu_{ik}) U_i^T$.
 - 7: Set weights $w_{ij} = (U_i(1, j))^2$ and compute $\eta_i = \sum_{j=1}^k w_{ij} f(\mu_{ij})$, where $f(\lambda) = \lambda - \ln \lambda - 1$.
 - 8: **end for**
 - 9: Estimate the trace: $\widehat{\text{tr}}(f(\mathcal{A})) = \frac{n}{q} \sum_{i=1}^q \eta_i$.
 - 10: **Output:** Estimated KL divergence $\hat{D}_{\text{KL}} = \frac{1}{2} \widehat{\text{tr}}(f(\mathcal{A}))$.
-

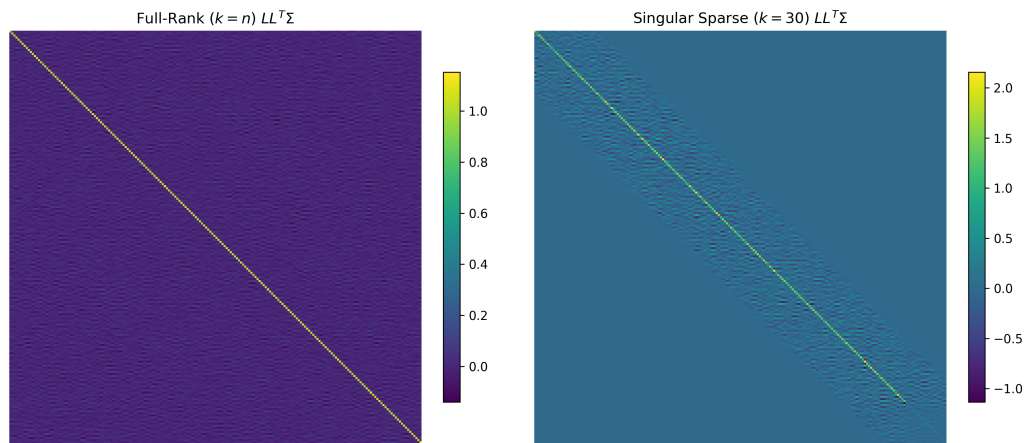


Figure 13: Full-Rank KL: 1.05
Singular Case KL: 81.0